Infrared, and Raman spectra, conformational stability, normal coordinate analysis, ab initio calculations, and vibrational assignment of 1-chlorosilacyclobutane

ARTICLE *in* JOURNAL OF MOLECULAR STRUCTURE THEOCHEM · APRIL 2000

Impact Factor: 1.37 · DOI: 10.1016/S0166-1280(00)00381-X

4 AUTHORS, INCLUDING:

Todor K Gounev
University of Missouri - Kansas City
77 PUBLICATIONS **576** CITATIONS
SEE PROFILE

Gamil A. Guirgis
College of Charleston
341 PUBLICATIONS **2,688** CITATIONS
SEE PROFILE

ELSEVIER

Journal of Molecular Structure (Theochem) 500 (2000) 275–291

THEO CHEM

www.elsevier.nl/locate/theochem

Infrared, and Raman spectra, conformational stability, normal coordinate analysis, ab initio calculations, and vibrational assignment of 1-chlorosilacyclobutane

J.R. Durig*, T.K. Gounev, P. Zhen[1], G.A. Guirgis[2]

Department of Chemistry, University of Missouri-Kansas City, 5100 Rockhill Road, Kansas City, MO 64110-2499, USA

Abstract

The infrared spectra (3500–40 cm^{-1}) of gaseous and solid and the Raman spectra (3500–30 cm^{-1}) of liquid and solid 1-chlorosilacyclobutane, c-C_3H_6SiClH, have been obtained. Both the axial and equatorial conformers with respect to the chlorine atom have been identified in the fluid phases. Variable temperature (−105 to −150°C) studies of the infrared spectra of the sample dissolved in liquid krypton have been carried out. From these data, the enthalpy difference has been determined to be 211 ± 17 cm^{-1} (2.53 ± 0.21 kJ/mol), with the equatorial conformer being the more stable form and the only conformer remaining in the annealed solid. At ambient temperatures, approximately 26% of the axial conformers are present in the vapor phase. A complete vibrational assignment is proposed for the equatorial conformer, and many of the fundamentals of the axial conformers have also been identified. The vibrational assignments are supported by normal coordinate calculations utilizing ab initio force constants. Complete equilibrium geometries, conformational stabilities, harmonic force fields, infrared intensities, Raman activities, and depolarization ratios have been determined for both rotamers by ab initio calculations employing the 6-31G(d) basis set at the levels of restricted Hartree–Fock (RHF) and/or Moller–Plesset (MP) to second order. Structural parameters have also been obtained using MP2/6-311+G(d,p) ab initio calculations. The r_0 parameters for both conformers are obtained from a combination of the ab initio predicted values and the twelve previously reported microwave rotational constants. The results are discussed and compared to those obtained for some similar molecules.

Keywords: Raman; Infrared; Conformational stability; Ab initio calculations; 1-chlorosilacyclobutane

1. Introduction

The cyclobutane molecule is puckered with D_{2d} symmetry but with a relatively low barrier to inversion [1,2]. Rather surprisingly, cyclobutane has a plastic solid phase, which probably arises, at least in part, because of the low barrier to inversion [3–9]. With monosubstitution of cyclobutane by a halogen atom (F, Cl, Br) or a methyl group, two conformers are possible in the fluid phases [10–21]. The axial conformers are in rather low abundance so in the initial

* Corresponding author. Tel.: + 1-816-235-1136; fax: + 1-816-235-5191.

E-mail address: jdurig@umkc.edu (J.R. Durig).

[1] Taken in part from the dissertation of P. Zhen which will be submitted to the Department of Chemistry in partial fulfillment of the PhD degree.

[2] Permanent address: Analytical R/D Department, Performance Products Division, Bayer, Bushy Park Plant, Charleston, SC 29411, USA.

0166-1280/00/$ - see front matter
PII: S0166-1280(00)00381-X

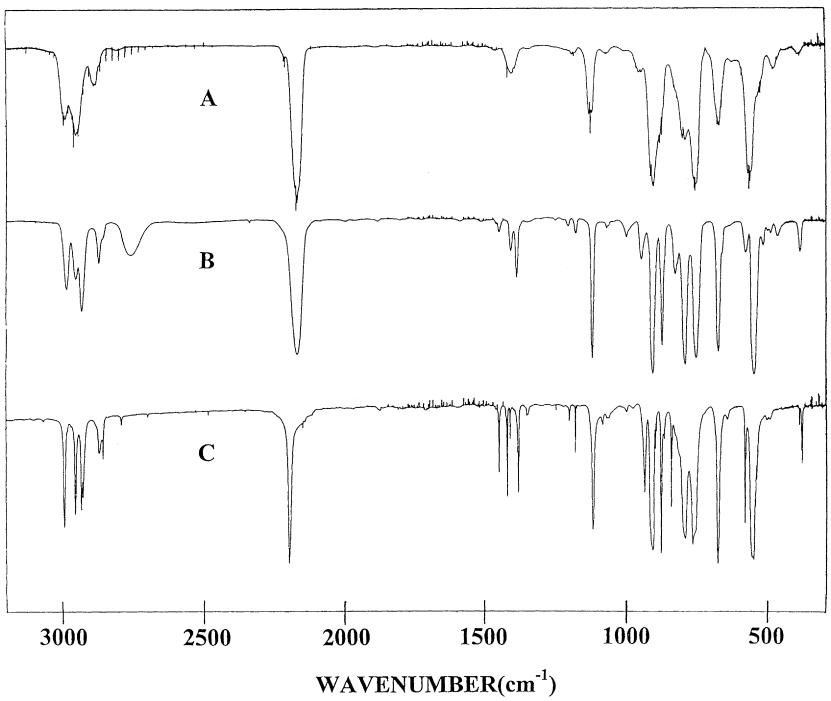

Fig. 1. Mid-infrared spectra of 1-chlorosilacyclobutane in (A) gas, (B) amorphous solid, (C) annealed solid.

vibrational [10–15] as well as microwave [22,23] studies of these molecules, results were reported only for the equatorial forms. In the more recent vibrational studies [18–21] some of the fundamentals of the axial forms have been observed. In addition, the microwave spectrum of the axial conformer of fluorocyclobutane [24] has also been reported. Even though the inversion barriers are similar to those in cyclobutane, none of these molecules has a plastic solid phase.

As a continuation of our conformational studies of the monohalocyclobutanes [18–21], we have initiated vibrational studies of the corresponding 1-halosilacyclobutane molecules. Not only are these investigations for the purposes of obtaining data for comparison with the corresponding substituted cyclobutane molecules but also for comparison to some recent studies of c-$C_3H_6Si(CH_3)X$ molecules [25–27]. Therefore, we have recorded the infrared spectra (3500–40 cm^{-1}) of gaseous and solid and the Raman spectra (3500–30 cm^{-1}) of liquid and solid 1-chlorosilacyclobutane. Additionally, variable temperature (−105 to −150°C) studies of the infrared spectra of the sample dissolved in liquid krypton have been carried out. From ab initio calculations employing the 6-31G(d) and 6-311+G(d,p) basis sets at the levels of restricted Hartree–Fock and/or with full electron correlation by the perturbation method to second order, complete equilibrium geometries, conformational stabilities, harmonic force fields, infrared intensities, Raman activities and depolarization ratios have been obtained. The results of this spectroscopic and theoretical investigation are reported herein.

2. Experimental

The sample was prepared in two steps. First the 1,1-dichlorosilacyclobutane [28] molecule was prepared and then it was reduced with lithium aluminum hydride in dry dibutyl ether. The product, silacyclobutane, was chlorinated using tin tetrachloride without solvent at room temperature for 18 h. The resulting 1-chlorosilacyclobutane was purified on a low-pressure, low-temperature fractionation column and the purity was checked by mass spectroscopy.

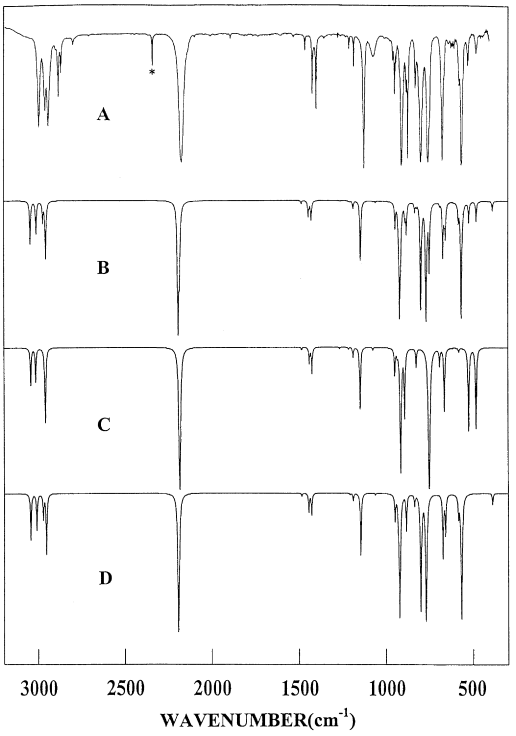

Fig. 2. Mid-infrared spectra of 1-chlorosilacyclobutane: (A) krypton solution at −145°C; (B) calculated spectrum of the mixture of both conformers; (C) calculated spectrum of the axial conformer; and (D) calculated spectrum of the equatorial conformer.

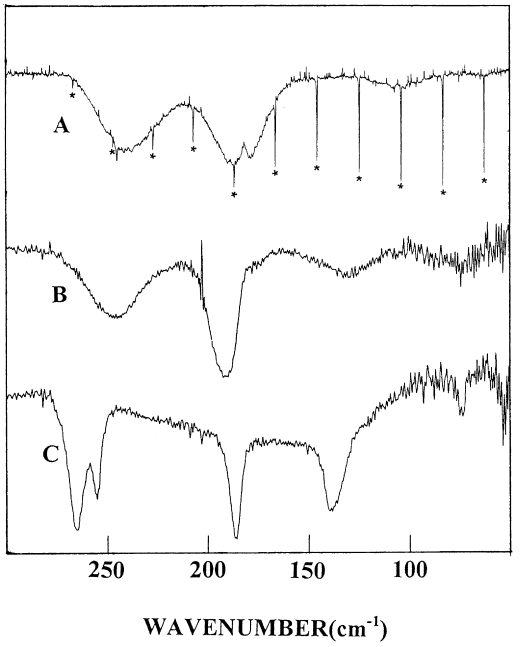

Fig. 3. Far infrared spectra of 1-chlorosilacyclobutane in the: (A) gas; (B) amorphous solid; and (C) annealed solid; sharp bands marked with asterisks are due to HCl impurity in spectrum of the gas.

The mid-infrared spectra of the gas and solid (Fig. 1) were obtained from 3200 to 300 cm^{-1} on a Perkin–Elmer model 2000 Fourier transform spectrometer equipped with a Ge/CsI beamsplitter and a DTGS detector. The gas was contained in a 10 cm cell fitted with CsI windows. This spectrum was obtained at a resolution of 0.5 cm^{-1} and transformed with boxcar truncation function. The spectrum of the solid was obtained by condensing the sample onto a liquid nitrogen cooled CsI plate contained in an evacuated cell equipped with CsI windows, and 256 scans were collected for both the reference and sample interferograms at 1 cm^{-1} resolution and then transformed with a boxcar truncation function. The sample was annealed until no further changes were noticeable in the spectra.

The mid-infrared spectra of the sample dissolved in liquified krypton (Fig. 2A) were recorded on a Bruker model IFS 66 Fourier transform spectrometer equipped with a globar source, a Ge/KBr beamsplitter and a DTGS detector. In all cases, 100 interferograms were collected at 1.0 cm^{-1} resolution, averaged and transformed with a boxcar truncation function. For these studies, a specially designed cryostat cell was used. It consisted of a copper cell with a pathlength of 4 cm with wedged silicon windows sealed to the cell with indium gaskets. The copper cell was enclosed in an evacuated chamber fitted with KBr windows. The temperature was maintained with boiling liquid nitrogen and monitored with two Pt thermoresistors. The complete cell was connected to a pressure manifold, allowing the filling and evacuation of the system. After cooling to the desired temperature, a small amount of the compound was condensed into the cell. Next, the system was pressurized with the noble gas, which immediately started to condense in the cell, allowing the compound to dissolve.

The far infrared spectrum of the gas (Fig. 3A) was recorded with a Bomem model DA3.002 Fourier transform spectrometer equipped with a vacuum bench, a 6.25 μm Mylar beamsplitter, and a liquid

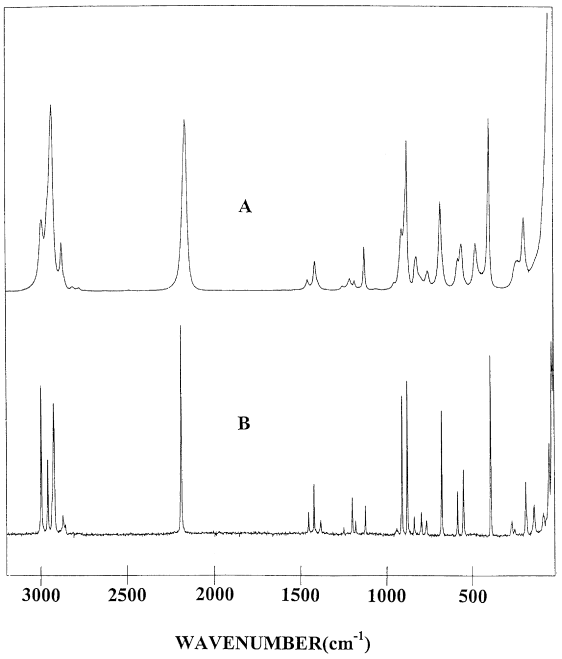

Fig. 4. Raman spectra of 1-chlorosilacyclobutane in (A) liquid and (B) annealed solid.

helium cooled Ge bolometer with a wedged sapphire filter and polyethylene window. The spectra were obtained from the sample contained in a 1 m folded path cell equipped with mirrors coated with gold, and fitted with polyethylene windows with an effective resolution of 0.10 cm^{-1}. To remove traces of water, an activated 4 Å molecular sieve was used to dry the sample. Interferograms were recorded 512 times at a resolution of 0.10 cm^{-1} and transformed with a boxcar truncation function. The spectra of the solids (Fig. 3B and C) were obtained with a Perkin–Elmer model 2000 spectrometer equipped with a metal grid beamsplitter and a DTGS detector.

The Raman spectra (Fig. 4) were recorded on a SPEX model 1403 spectrophotometer equipped with a Spectra-Physics model 164 argon ion laser operating on the 514.5 nm line. The laser power used was 0.5 W with a spectral bandpass of 3 cm^{-1}. The spectrum of the liquid was recorded with the sample sealed in a Pyrex glass capillary held in a Miller–Harney apparatus [29]. Depolarization measurements were obtained for the liquid sample using a standard Ednalite 35 mm camera polarizer with 38 mm of free aperture affixed to the SPEX instrument. Depolarization ratio measurements were checked by measuring the state of polarization of the Raman bands of CCl_4 immediately before measurements were made on the liquid sample. The reported Raman frequencies are expected to be accurate to ± 2 cm^{-1}. The Raman spectrum of the solid was obtained by cooling the sample capillary with chilled nitrogen vapors until the sample solidified. All of the observed bands in both the infrared and Raman spectra, along with the proposed assignments, are listed in Table 1.

3. Ab initio calculations

The LCAO–MO–SCF restricted Hartree–Fock calculations were performed with the GAUSSIAN-94 program [30] using Gaussian-type basis functions. The energy minima with respect to nuclear coordinates were obtained by the simultaneous relaxation of all of the geometric parameters consistent with the symmetry restrictions using the gradient method of Pulay [31]. The structural optimization for both the equatorial and the axial conformers were carried out with initial parameters taken from those of 1-chloro-1-methylsilacyclobutane [25]. The 6-31G(d) and 6-311+G(d,p) basis sets were employed at the level of restricted Hartree–Fock (RHF) and/or Moller–Plesset (MP2) to second order. The determined structural parameters are listed in Table 2.

In order to obtain a more complete description of the molecular motions involved in the normal modes of 1-chlorosilacyclobutane, we have carried out a normal coordinate analysis. The force fields in Cartesian coordinates were calculated by the GAUSSIAN-94 program [30] with the MP2/6-31G(d) basis set. The internal coordinates used to calculate the G and B matrices are listed in Table 2. Using the B matrix, the force field in Cartesian coordinates was converted to a force field in internal coordinates and the pure ab initio vibrational frequencies were reproduced. The force constants for both the axial and equatorial conformers can be obtained from the authors. Subsequently, a scaling factor of 0.9 for all modes was used to obtain the fixed scaled force field and resultant wavenumbers. A set of symmetry coordinates was used (Table 3) to determine the corresponding potential energy distributions (PED). A comparison between the observed and calculated wavenumbers

Table 1
Observed infrared (abbreviations used: s, strong; m, moderate; w, weak; v, very; bd, broad; sh, shoulder; p, polarized; dp, depolarized; A, B, and C refer to infrared band envelopes; P, Q, and R refer to the rotational–vibrational branches) and Raman wavenumbers (cm^{-1}) for 1-chlorosilacyclobutane

Infrared						Raman				Assignment	
Gas	Rel. int.	Krypton solution	Rel. int	Solid	Rel. int.	Liquid	Rel. int. & Depol.	Solid	Rel. int.	ν_i [a]	Approximate description
3002 R											
2997 Q C	m	2993	s	2996	s	2990	m,p	2999	s	$\nu_1\nu_{19}$	$(CH_2)_2$ antisymmetric stretch
2991 P											
2966 Q	m									ν_2'	CH_2 antisymmetric stretch
2962 Q	s	2957	s	2957	s	2956	sh,m,p	2961	m	ν_2	CH_2 antisymmetric stretch
2947 max	s	2940	s	2935	s	2934	vs,p	2936	sh,w	$\nu_3\nu_{20}$	$(CH_2)_2$ symmetric stretch
2937 max	sh m			2929	m			2927	s	ν_4	CH_2 symmetric stretch
2889 max	w	2879	m	2871	w	2879	w,p	2875	vw		$(\nu_6 + \nu_7)$
		2865	w	2858	w			2861	vw		
2175 R											
2172 Q	vs	2169	vs	2199	vs	2168	vs,p	2195	vs	ν_5	Si–H stretch
2168 Q,A/C	vs									ν_5'	Si–H stretch
2161 P											
1466 R											
1461 Q,A/C	vw	1455	vw	1452	m	1456	vw,p	1456	vw	ν_6	CH_2 deformation
1455 P											
1421 Q,C	w	1415	m	1423	s	1413	w,dp	1424	m	ν_7	$(CH_2)_2$ deformation
				1412	w						
1406 R											
1398 min B	w	1394	m	1383	s	1397	sh,vw,dp	1387	vw	ν_{21}	$(CH_2)_2$ deformation
1395 P											
1345 max	vw	1349	vw	1349	vw						$(\nu_{13} + \nu_{15})$
		1257	vw							ν_{22}'	CH_2 wag
1248	vw	1253	vw	1250	vw	1254	vw,dp	1253	vw	ν_{22}	CH_2 wag
1214 R		1228	vw								
1210 min B	vw	1209	vw	1203	vw	1212	vw,dp	1203	w	ν_{23}	CH_2 twist
1205 P											
1191 R											
1186 Q,A/C	vw	1183	w	1183	w	1183	vw,p	1184	vw	ν_8	$(CH_2)_2$ twist
1179 P											
1134 R		1129	sh,s							ν_9'	$(CH_2)_2$ wagt
1128 Q,A/C	m	1125	vs	1121	vs	1126	w,p	1126	w	ν_9	$(CH_2)_2$ wag
1123 P											
				1087	vw						Combination
1072 max	vw	1074	bd,vw	1071	vw	1065	bd,vw,dp	1069	vw	ν_{24}	$(CH_2)_2$ wag
				1065	vw						
				1002	vw						
966 Q	vw	962	w	980	vw						$(\nu_{15} + \nu_{16})$

Table 1 (*continued*)

Infrared						Raman				Assignment	
Gas	Rel. int.	Krypton solution	Rel. int	Solid	Rel. int.	Liquid	Rel. int. & Depol.	Solid	Rel. int.	ν_i [a]	Approximate description
958 R											
953 min B	w	952	m	947	sh,w	954	sh,vw,dp			ν_{25}	$(CH_2)_2$ twist
948 P											
		943	w	938	s			943	vw	ν_{26}	C–C ring stretch
918 Q,A/C	s	924	sh,w	918	sh,vs						
916 Q,A/C	s	912	vs	909	vs	921	sh,vw,p	911	s	ν_{10}	CH_2 rock
909 R											
906 Q,A/C		904	sh,m			908	m,p			ν'_{10}	CH_2 rock
				900	vw						$(\nu_{13} + \nu_{18})$ or $(\nu_{17} + \nu_{28})$
				897	vw						
886 Q	s	886	m			887	sh,m,p			ν'_{11}	C–C ring stretch
878 Q,A	s	877	vs	880	vs	880	s,p	881	s	ν_{11}	C–C ring stretch
872 P											
		872	m	869	w						$(\nu_{13} + \nu_{18})$ or $(\nu_{14} + \nu_{30})$
835 max	w	833	m	844	s			841	vw	ν_{12}	$(CH_2)_2$ rock
				841	w						
823Q,A/C	w	812	sh,w			824	w,p			ν'_{12}	$(CH_2)_2$ rock
806 R											
802 min B	m	801	vs	794	vs	804	sh,w,dp	798	vw	ν_{27}	Si–H out-of-plane-bend
796 P											
766 R											
764 Q,A/C	vs										
761 Q,A/C	vs	759	vs	768	vs	758	vw,p	768	vw	ν_{13}	Si–H in plane bend
756 P				757	vs						
749 max	s	751	sh,s			751	sh,vw,p			ν'_{13}	Si–H in plane bend
688 R											
683 Q,A/C	m	677	vs	679	vs	682	m,p	679	s	ν_{14}	Si–C ring stretch
678 P				676	sh,vs						
674	m	667	w							ν'_{14}	Si–C ring stretch
667 max	m	663	sh,vw	669	vw	663	sh,w,dp			ν_{28}	Si–C ring stretch
595 max	sh,w	580	m	583	s	580	w,dp	587	w	ν_{29}	$(CH_2)_2$ rock
575 R											
571 Q,A/C	vs	567	vs								
567 Q,A/C	vs	562	vs	559	vs	560	w,p	552	m	ν_{15}	Si–Cl^{35} stretch
562 P		558	s	553	vs						Si–Cl^{37} stretch
538 R											
534 Q,A/C	w										
530 Q,A/C	w	528	w							ν'_{16}	ring deformation
				507	vw						$2\nu_{17}$
				496	vw						

Table 1 (*continued*)

Infrared						Raman				Assignment	
Gas	Rel. int.	Krypton solution	Rel. int	Solid	Rel. int.	Liquid	Rel. int. & Depol.	Solid	Rel. int.	ν_i [a]	Approximate description
525 P											
480 R		480	vw			477	w,p			ν'_{15}	Si–Cl^{35} stretch
474 Q,A/C	w	473	vw							ν'_{15}	Si–Cl^{37} stretch
471 P											
397 max	vw			394	vw	399	vs,p	394	vs	ν_{16}	ring deformation
				387	w						
				385	m						
245 Q	m			265	m	242	w,p	270	vw	ν_{17}	ring puckering
				255	w			253	vw		
186 R											
182 min B	m			186	m	193	m,dp	189	m	ν_{30}	Si–Cl out-of-plane bend
177 P											
107	vw			139	w			140	w	ν_{18}	Si–Cl in-plane bend
				73	vw			84	vw		lattice mode
				40	vw			51	m		lattice mode
								33	s		lattice mode

[a] ν_i and ν'_i refer to the equatorial and axial conformers, respectively.

Table 2
Structural parameters (bond distances in Å, bond angles in degrees, rotational constants in MHz, dipole moments in Debye, and energies in Hartrees) rotational constants, dipole moments and energy for molecule 1-chlorosilacyclobutane

		RHF/6-31G(d)		MP2/6-31G(d)		MP2/6-311+G(d,p)		r_0 adjusted[a]	
Parameter	Internal coordinate	Equatorial	Axial	Equatorial	Axial	Equatorial	Axial	Equatorial	Axial
Si–C_2(C_3)	R_1,R_2	1.882	1.883	1.881	1.883	1.873	1.878	1.871	1.875
Si–H	r_7	1.471	1.471	1.485	1.486	1.474	1.475	1.484	1.485
Si–Cl	R_5	2.074	2.077	2.067	2.070	2.061	2.068	2.051	2.058
C_4–C_2(C_3)	R_3, R_4	1.565	1.564	1.561	1.560	1.563	1.565	1.564	1.565
C–H_7(H_9)	r_1,r_3	1.083	1.087	1.092	1.096	1.090	1.096	1.090	1.096
C–H_8(H_{10})	r_2,r_4	1.085	1.082	1.095	1.092	1.094	1.091	1.094	1.091
C–H_5	r_5	1.085	1.084	1.095	1.095	1.095	1.094	1.095	1.094
C–H_6	r_6	1.084	1.084	1.094	1.094	1.093	1.094	1.093	1.094
∠CSiC	θ_1	79.85	79.93	79.27	79.25	79.55	79.44	80.40	80.29
∠CCSi	α_1,β_1	86.50	87.32	85.32	86.48	85.25	86.10	85.41	87.21
∠$C_2C_4C_3$	ν_1	101.0	101.3	100.5	100.7	100.1	100.1	101.1	101.1
∠H_{11}SiCl	θ_2	106.2	105.8	106.9	106.3	106.7	106.0	106.7	106.0
∠SiCH_7(H_9)	α_2,β_2	121.2	111.9	122.0	111.1	122.3	111.1	122.6	111.1
∠SiCH_8(H_{10})	α_3,β_3	112.3	121.0	111.6	121.7	111.1	121.8	111.1	122.2
∠CCH_7(H_9)	α_5,β_5	115.7	111.6	116.5	111.1	116.6	110.5	118.3	104.7
∠CCH_8(H_{10})	α_6,β_6	111.1	115.4	110.5	116.2	110.1	116.3	107.5	120.1
∠CCH_5	ν_2,ν_4	110.2	113.9	110.1	114.4	110.1	114.4	109.9	114.1
∠CCH_6	ν_3,ν_5	113.9	110.0	114.3	109.7	114.3	109.8	114.0	109.6
∠$H_5C_4H_6$	ν_6	107.5	107.6	107.5	107.7	107.9	108.1	107.9	108.1
∠$H_7C_2H_8$	α_4	108.5	108.3	109.0	108.6	109.4	109.2	109.4	109.2
∠$H_9C_3H_{10}$	β_4	108.5	108.3	109.0	108.6	109.4	109.2	109.4	109.2
∠CSiCl	φ_1,φ_2	118.5	113.8	120.1	112.6	119.9	111.4	119.6	111.1
∠CSiH_{11}	δ_1,δ_2	116.2	121.1	114.4	122.2	114.6	123.4	144.5	123.3
Puckering angle		27.1	22.2	33.9	29.1	34.4	31.3	30.4	22.3
τ($C_4SiH_{11}Cl$)		180.0	180.0	180.0	180.0	180.0	180.0	180.0	180.0
A		7386	6067	7616	5900	7648	5801	7536[b]	5927[b]
B		1858	2011	1844	2060	1857	2100	1878[b]	2083[b]
C		1683	1905	1667	1977	1678	2029	1693[b]	1988[b]
$\lvert\mu_a\rvert$		1.314	0.878	1.339	0.761	1.265	0.659		
$\lvert\mu_b\rvert$		0.000	0.000	0.000	0.000	0.000	0.000		
$\lvert\mu_c\rvert$		1.945	2.256	1.814	2.219	1.719	2.172		
$\lvert\mu_t\rvert$		2.347	2.421	2.255	2.346	2.134	2.270		
$-(E + 866)$		0.113952	0.113270	0.711672	0.710379	0.1907513	0.1898302		
ΔE (cm^{-1})			150		284		202		

[a] Calculated using the rotational constants reported in Ref. [39].
[b] Calculated values corresponding to the r_0 adjusted parameters.

Table 3
Symmetry coordinates (not normalized) for 1-chlorosilacyclobutane

Species	Description	Symmetry coordinate
A′	$(CH_2)_2$ antisymmetric stretch	$S_1 = r_2 - r_1 + r_4 - r_3$
	CH_2 antisymmetric stretch	$S_2 = r_5 - r_6$
	$(CH_2)_2$ symmetric stretch	$S_3 = r_1 + r_2 + r_3 + r_4$
	CH_2 symmetric stretch	$S_4 = r_5 + r_6$
	Si–H stretch	$S_5 = r_7$
	CH_2 deformation	$S_6 = 4\nu_6 - \nu_2 - \nu_3 - \nu_4 - \nu_5$
	$(CH_2)_2$ deformation	$S_7 = 4\alpha_4 + 4\beta_4 - \alpha_2 - \alpha_3 - \alpha_5 - \alpha_6 - \beta_2 - \beta_3 - \beta_5 - \beta_6$
	$(CH_2)_2$ twist	$S_8 = \alpha_2 - \alpha_3 - \alpha_5 + \alpha_6 + \beta_2 - \beta_3 - \beta_5 + \beta_6$
	$(CH_2)_2$ wag	$S_9 = \alpha_2 + \alpha_3 - \alpha_5 - \alpha_6 + \beta_2 + \beta_3 - \beta_5 - \beta_6$
	CH_2 rock	$S_{10} = \nu_3 - \nu_2 + \nu_5 - \nu_4$
	C–C ring stretch	$S_{11} = R_3 + R_4$
	$(CH_2)_2$ rock	$S_{12} = \alpha_2 - \alpha_3 + \alpha_5 - \alpha_6 + \beta_2 - \beta_3 + \beta_5 - \beta_6$
	Si–H in-plane bend	$S_{13} = 2\theta_2 - \delta_1 - \delta_2$
	Si–C ring stretch	$S_{14} = R_1 + R_2$
	Si–Cl stretch	$S_{15} = R_5$
	Ring deformation	$S_{16} = \alpha_1 + \beta_1 - \nu_1 - \theta_1$
	Ring puckering	$S_{17} = \alpha_1 + \beta_1 + \nu_1 + \theta_1$
	Si–Cl in-plane bend	$S_{18} = \varphi_1 + \varphi_2$
A″	$(CH_2)_2$ antisymmetric stretch	$S_{19} = r_2 - r_1 + r_3 - r_4$
	$(CH_2)_2$ symmetric stretch	$S_{20} = r_1 + r_2 - r_3 - r_4$.
	$(CH_2)_2$ deformation	$S_{21} = 4\alpha_4 - \alpha_2 - \alpha_3 - \alpha_5 - \alpha_6 - 4\beta_4 + \beta_2 + \beta_3 + \beta_5 + \beta_6$
	CH_2 wag	$S_{22} = \nu_4 + \nu_5 - \nu_2 - \nu_3$
	CH_2 twist	$S_{23} = \nu_2 - \nu_3 - \nu_4 + \nu_5$
	$(CH)_2$ wag	$S_{24} = \alpha_5 + \alpha_6 - \alpha_2 - \alpha_3 + \beta_2 + \beta_3 - \beta_5 - \beta_6$
	$(CH_2)_2$ twist	$S_{25} = \alpha_3 - \alpha_2 + \alpha_5 - \alpha_6 + \beta_2 - \beta_3 - \beta_5 + \beta_6$
	C–C ring stretch	$S_{26} = R_3 - R_4$
	Si–H out-of-plane bend	$S_{27} = \delta_1 - \delta_2$
	Si–C ring stretch	$S_{28} = R_1 - R_2$
	$(CH_2)_2$ rock	$S_{29} = \alpha_3 - \alpha_2 - \alpha_5 + \alpha_6 + \beta_2 - \beta_3 + \beta_5 - \beta_6$
	Si–Cl out-of-plane bend	$S_{30} = \varphi_1 - \varphi_2$

of 1-chlorosilacyclobutane along with the calculated infrared intensities, Raman activities, depolarization ratios and PED are given in Table 4.

To aid in the vibrational assignment, Raman and infrared spectra for 1-chlorosilacyclobutane were calculated using the predicted wavenumbers, scattering activities and intensities determined from the ab initio calculations. The evaluation of Raman activity by using the analytical gradient methods has been previously developed [32,33]. The activity S_j can be expressed as:

$$S_j = g_j(45\alpha_j^2 + 7\beta_j^2)$$

where g_j is the degeneracy of the vibrational mode j, α_j is the derivative of the isotropic polarizability and β_j is that of the anisotropic polarizability. The Raman scattering cross-sections, $\partial\sigma_j/\partial\Omega$, which are proportional to the Raman intensities, can be calculated from the scattering activities and the predicted frequencies

Table 4
Observed and calculated frequencies (cm^{-1}) for equatorial and axial 1-chlorosilacyclobutane

Species	Vib. no.	Description	Equatorial							Axial						
			Ab initio[a]	Fixed Scaled[b]	IR int.[c]	Raman act.[d]	dp ratio[d]	Obs.	P.E.D.[f]	Ab initio[a]	Fixed Scaled[b]	IR int[c]	Raman act[d]	dp ratio[d]	Obs.[e]	P.E.D.[f]
A′	ν_1	$(CH_2)_2$ antisymmetric stretch	3210	3045	10.3	81.3	0.54	2997	$91S_1$	3207	3043	9.7	82.4	0.48		$83S_1,10S_3$
	ν_2	CH_2 antisymmetric stretch	3173	3010	14.7	109.3	0.27	2962	$92S_2$	3177	3014	13.7	87.4	0.38	2966	$91S_2$
	ν_3	$(CH_2)_2$ symmetric stretch	3134	2973	1.5	194.9	0.16	2947	$91S_3$	3122	2962	4.8	168.7	0.09		$80S_3,13S_1$
	ν_4	CH_2 symmetric stretch	3115	2955	27.5	80.3	0.35	2937	$99S_4$	3119	2958	30.8	119.7	0.37		$94S_4$
	ν_5	Si–H stretch	2311	2193	152.0	130.0	0.19	2172	$100S_5$	2303	2185	191.4	150.2	0.20	2168	$100S_3$
	ν_6	CH_2 deformation	1564	1484	1.1	6.8	0.72	1461	$94S_6$	1562	1482	0.9	6.7	0.71		$94S_6$
	ν_7	$(CH_2)_2$ deformation	1522	1444	7.0	20.3	0.75	1421	$94S_7$	1517	1439	6.0	21.3	0.75		$93S_7$
	ν_8	$(CH_2)_2$ twist	1255	1191	2.7	4.4	0.62	1186	$46S_8,24S_{10},15S_{12},14S_9$	1254	1190	3.7	4.6	0.64		$47S_8,24S_{10},15S_{12},12S_9$
	ν_9	$(CH_2)_2$ wag	1210	1148	28.5	2.9	0.69	1128	$68S_9,11S_8,10S_{11}$	1212	1150	28.6	2.6	0.65	(1129)	$69S_9,10S_8,10S_{11}$
	ν_{10}	CH_2 rock	973	923	97.7	15.2	0.15	917	$19S_{10},19S_{11},$ $19S_{13},17S_8,15S_{12}$	966	917	101.8	16.4	0.22	906	$24S_{10},23S_{13},22S_8,14S_{12}$
	ν_{11}	C–C ring stretch	932	884	14.8	16.8	0.18	878	$61S_{11},13S_8,10S_{14}$	942	894	33.2	14.1	0.05	886	$75S_{11},10S_{14}$
	ν_{12}	$(CH_2)_2$ rock	883	837	4.0	3.0	0.03	835	$16S_{12},24S_{10},23S_{14},19S_{16}$	871	827	7.2	4.6	0.09	823	$21S_{12},24S_{16},23S_{14}18_{10},10S_9$
	ν_{13}	Si–H in-plane bend	811	770	106.3	4.3	0.68	763	$68S_{13}$	794	753	82.7	5.8	0.62	749	$59S_{13},15S_{10},15S_8$
	ν_{14}	Si–C ring stretch	711	674	29.7	4.6	0.18	683	$41S_{14},24S_{10},21S_{12}$	701	665	29.8	6.0	0.53	674	$36S_{14},25S_{12},13S_{10},11S_{15},10S_{13}$
	ν_{15}	Si–Cl stretch	597	566	100.8	4.6	0.29	571	$59S_{15},26S_{16}$	508	482	41.9	10.7	0.17	470	$53S_{15},19S_{14},19S_{16}$
	ν_{16}	Ring deformation	409	388	4.2	9.9	0.26	397	$40S_{16},32S_{15},19S_{14}$	552	524	43.7	3.0	0.64	534	$50S_{16},32S_{15}$
	ν_{17}	Ring puckering	265	251	3.7	1.2	0.67	246	$47S_{17},35S_{18},11S_{12}$	242	230	0.7	2.1	0.45		$43S_{17},36S_{18},13S_{12}$
	ν_{18}	Si–Cl in-plane bend	125	118	1.9	0.8	0.54	104	$56S_{18},42S_{17}$	114	108	1.0	0.6	0.74		$53S_{18},45S_{17}$
A″	ν_{19}	$(CH_2)_2$ antisymmetric stretch	3210	3045	9.3	102.7	0.75	2997	$93S_{19}$	3207	3042	6.2	90.5	0.75		$88S_{19},12S_{20}$
	ν_{20}	$(CH_2)_2$ symmetric stretch	3134	2973	7.9	11.0	0.75	2947	$93S_{20}$	3121	2960	7.0	28.3	0.75		$88S_{20},12S_{19}$
	ν_{21}	$(CH_2)_2$ deformation	1505	1428	8.1	5.3	0.75	1397	$99S_{21}$	1501	1424	10.1	5.3	0.75		$99S_{21}$
	ν_{22}	CH_2 wag	1330	1262	0.1	1.9	0.75	(1253)	$74S_{22},13S_{23}$	1336	1267	0.5	0.9	0.75	(1275)	$79S_{22}$
	ν_{23}	CH_2 twist	1276	1210	0.5	8.6	0.75	1212	$52S_{23},23S_{24}$	1281	1216	0.7	10.6	0.75		$59S_{23},19S_{24}$
	ν_{24}	$(CH_2)_2$ wag	1120	1063	0.6	2.0	0.75	1072	$71S_{24}$	1134	1076	1.0	1.4	0.75		$74S_{24}$
	ν_{25}	$(CH_2)_2$ twist	1001	950	9.9	2.3	0.75	953	$63S_{25},22S_{23}$	1003	951	10.3	8.4	0.75		$35S_{25},42S_{26}$
	ν_{26}	C–C ring stretch	983	932	6.1	7.9	0.75	(943)	$86S_{26}$	988	937	1.9	2.4	0.75		$45S_{26},34S_{25},16S_{23}$
	ν_{27}	Si–H out-of-plane bend	843	800	84.0	3.2	0.75	802	$54S_{27},30S_{29}$	792	752	107.7	1.9	0.75	749	$63S_{27},27S_{28}$
	ν_{28}	Si–C ring stretch	695	659	16.6	7.2	0.75	667	$82S_{28}$	612	581	1.5	4.8	0.75		$43S_{28},29S_{29},20S_{27}$
	ν_{29}	$(CH_2)_2$ rock	616	584	7.9	3.9	0.75	(580)	$50S_{29},34S_{27}$	730	693	6.5	7.7	0.75		$53S_{29},23S_{28},11S_{27}$
	ν_{30}	Si–Cl out-of-plane bend	186	177	2.9	1.9	0.75	182	$94S_{30}$	191	182	2.0	2.0	0.75		$93S_{30}$

[a] Calculated with the MP2/6-31G* basis set.
[b] Scaling factors of 0.9 for stretching and bending coordinates.
[c] Calculated infrared intensities in km/mol.
[d] Calculated Raman activities in $Å^4$/amu, using RHF/6-31G* basis set.
[e] Frequencies are taken from the infrared spectrum of the gas, except the ones in parentheses, which are taken from the infrared spectrum of the solid.
[f] For a description of the symmetry coordinates see Table 3.

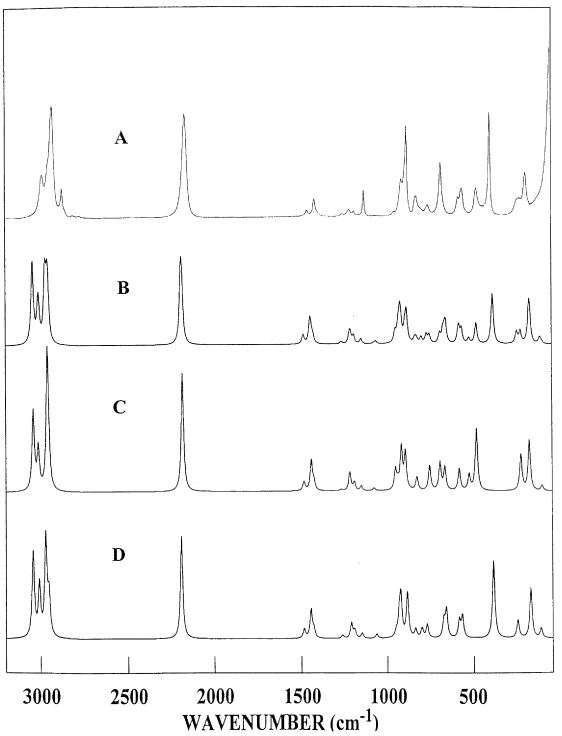

Fig. 5. Raman spectra of 1-chlorosilacyclobutane: (A) experimental spectrum of the liquid; (B) calculated spectrum of the mixture of both conformers; (C) calculated spectrum of the axial conformer; and (D) calculated spectrum of the equatorial conformer.

for each normal mode using the relationship [34,35]:

$$\frac{\partial\sigma_j}{\partial\Omega} = \left(\frac{2^4\pi^4}{45}\right)\left(\frac{(\nu_0 - \nu_j)^4}{1 - \exp\left[\frac{-\mathrm{h}c\nu_j}{\mathrm{k}T}\right]}\right)\left(\frac{\mathrm{h}}{8\pi^2 c\nu_j}\right)S_j$$

where ν_0 is the exciting frequency, ν_j the vibrational frequency of the jth normal mode, h, c and k are universal constants, and S_j is the corresponding Raman scattering activity. To obtain the polarized Raman scattering cross-section, the polarizabilities are incorporated into S_j by $S_j[(1-\rho_j)/(1+\rho_j)]$ where ρ_j is the depolarization ratio of the jth normal mode. The Raman scattering cross-sections and calculated fixed scaled frequencies are used together with a Lorentzian line shape function to obtain the calculated spectrum. The predicted Raman spectra of the pure axial and equatorial conformers are shown in Fig. 5C and D, respectively. The predicted Raman spectrum of the mixture of the two conformers with a ΔH value of 211 cm^{-1} is shown in Fig. 5B which should be compared to the experimental spectrum of the liquid (Fig. 5A). The ΔH value utilized is the value obtained from the temperature dependent study of the spectra of the krypton solution.

Infrared intensities were also calculated based on the dipole moment derivatives with respect to the Cartesian coordinates. The derivatives were taken from the ab initio calculations at the MP2/6-31G(d) level and transformed to normal coordinates by:

$$\left(\frac{\partial\mu_\mu}{\partial Q_i}\right) = \sum_j \left(\frac{\partial\mu_\mu}{\partial X_j}\right)L_{ji}$$

where the Q_i is the ith normal coordinate, X_j is the jth Cartesian displacement coordinate, and L_{ji} is the transformation matrix between the Cartesian displacement coordinates and normal coordinates. The infrared intensities were then calculated by

$$I_i = \frac{N\pi}{3c^2}\left[\left(\frac{\partial\mu_x}{\partial Q_i}\right)^2 + \left(\frac{\partial\mu_y}{\partial Q_i}\right)^2 + \left(\frac{\partial\mu_z}{\partial Q_i}\right)^2\right]$$

The predicted infrared spectra of the axial and equatorial conformers are shown in Fig. 2C and D, respectively. The combination of the spectra of the two conformers with a ΔH of 211 cm^{-1} is shown in Fig. 2B and the experimental spectrum of the sample dissolved in liquid krypton is shown in Fig. 2A for comparison. These spectra were very useful for determining the bands to be used for the determination of the enthalpy difference.

4. Conformational stability

There are several examples in both the Raman and infrared spectra, which show that there are more than one conformer of 1-chlorosilacyclobutane present in the fluid phases. For example, the polarized band at 477 cm^{-1} in the Raman spectrum of the liquid completely disappears in the Raman spectrum of the polycrystalline solid (Fig. 4). In the infrared spectra (Fig. 1), the gas phase bands at 530 and 474 cm^{-1} remain in the spectrum of the amorphous solid but disappear upon crystallization of the sample. These bands are confidently assigned to fundamentals of the axial conformer since the ab initio calculations

Table 5
Temperature and intensity ratio for the conformational study of 1-chloro-1-silacyclobutane ($\Delta H = 211 \pm 17$ with the equatorial conformer more stable)

T/°C	1000/T (K)	$K = I_{877(eq)}/I_{477(ax)}$	$-\ln k$	$K = I_{877(eq)}/I_{528}$(ax)	$-\ln k$	$K = I_{678(eq)}/I_{477(ax)}$	$-\ln k$	$K = I_{678(eq)}/I_{528(ax)}$	$-\ln k$
−105	5.95	2.513	−0.922	2.702	−0.994	5.101	−1.629	5.483	−1.702
−115	6.32	2.879	−1.057	3.042	−1.113	6.110	−1.810	6.457	−1.865
−120	6.53	3.813	−1.338	3.752	−1.322	7.757	−2.049	7.633	−2.033
−125	6.75	3.674	−1.301	4.155	−1.424	7.375	−1.998	8.342	−2.121
−130	6.99	4.496	−1.503	3.963	−1.377	8.820	−2.177	7.775	−2.051
−135	7.24	3.757	−1.324	4.909	−1.591	7.469	−2.011	9.758	−2.278
−140	7.51	4.806	−1.570	4.089	−1.408	9.650	−2.267	8.210	−2.105
−145	7.80	5.288	−1.665	4.600	−1.526	10.835	−2.383	9.426	−2.243
−150	8.12	5.812	−1.760	5.027	−1.615	11.524	−2.445	9.967	−2.299
ΔH (cm^{-1})			253 ± 33		180 ± 36		243 ± 32		170 ± 33

clearly show that they are the only bands expected in this spectral region. From these data, it is also concluded that the equatorial conformer is the only form present in the polycrystalline solid.

In order to determine the enthalpy difference, ΔH, between the conformers of 1-chlorosilacylcobutane, the relative band intensities of the conformer bands at 877, 678, 528 and 477 cm^{-1} in the infrared spectrum of the sample dissolved in liquid krypton were measured as a function of temperature. The first two bands belong to the equatorial conformer, whereas the other two belong to the axial conformer. Nine sets of data were obtained for these four bands in the temperature range from −105 to −150°C (Table 5). The intensity data for the conformer bands were fit to the van't Hoff equation $-\ln K = (\Delta H/RT) - (\Delta S/R)$, where K is substituted with the intensity ratio (I_{eq}/I_{ax}), and it is assumed that ΔH is not a function of temperature. Using a least-squares fit of the slope of the van't Hoff plot, an average ΔH value of 211 ± 17 cm^{-1} (2.53 ± 0.21 kJ/mol) was obtained with the equatorial conformer the more stable form. This value should be representative of ΔH in the gas phase [36–40], since the molecular size and dipole moments of both conformers are almost the same. At ambient temperature there is approximately 26% of the axial conformer present in the vapor state.

5. Vibrational assignment

Both the axial and equatorial conformers of 1-chlorosilacyclobutane have a plane of symmetry and the 30 normal modes span the representations of 18 A′ and 12 A″ species of the C_s symmetry group. The A′ vibrations are expected to produce polarized Raman lines and A, C or A/C type hybrid band contours. The A″ modes should give rise to depolarized lines in the Raman spectrum and yield B-type infrared band envelops. Thus to identify the A′ and A″ vibrations, we utilized the measured depolarization ratios and observed infrared band contours, whereas to distinguish between the equivalent modes of the two conformers we relied on the predicted wavenumber order, infrared intensities and Raman activities from the ab initio calculations.

The $(CH_2)_2$ antisymmetric stretches produce the C-type Q-branch at 2997 cm^{-1}, whereas the corresponding symmetric stretches are assigned to the strong band at 2940 cm^{-1} in the spectrum of the krypton solution. The bands at 2961 and 2927 cm^{-1} in the Raman spectrum of the solid are associated with the CH_2 antisymmetric and symmetric stretches, respectively. The band at 2889 is assigned as an overtone in Fermi resonance with the nearby stretching fundamental. The Si–H stretches of the equatorial and axial conformers give rise to the very strong Q-branches located at 2172 and 2168 cm^{-1}, respectively, in the infrared spectrum of the gas.

The intensities of the bands in the carbon–hydrogen deformational region are quite low in both the infrared and Raman spectra. Nevertheless, the $(CH_2)_2$ deformations are observed in the Raman spectrum of the liquid at 1413 and 1397 cm^{-1}, whereas, the CH_2 deformation is located at 1461 cm^{-1} in the infrared spectrum of the gas. The CH_2 wagging and twisting fundamentals are both in the A″ symmetry block and are very weak B-type bands in the infrared spectrum of the gas. In the Raman spectrum of the liquid, they produce two weak depolarized bands at 1254 and 1212 cm^{-1}. In the infrared spectrum of the gas, A/C type bands are observed for the A′ $(CH_2)_2$ twist and wag at 1186 and 1128 cm^{-1}. The corresponding A″ wag and twist, ν_{24} and ν_{25}, yield the B-type bands at 1072 and 953 cm^{-1}, respectively.

The cluster of bands around 900 cm^{-1} is associated with the various CC ring stretches and CH_2 rocks of the two conformers. The sharp A/C type Q-branches at 916 and 906 cm^{-1} are assigned to the CH_2 rocks of the equatorial and axial conformers, respectively. The latter band is not observed in the spectra of the annealed solid. The A″ CC ring stretch is apparent in the infrared spectrum of the solid at 938 cm^{-1}, whereas the respective A′ vibration shows a doublet for the two conformers in the Raman spectrum of the liquid at 877/880 cm^{-1} with the second component remaining in the Raman spectrum of the solid at 881 cm^{-1}. This second component is assigned to the equatorial form. A B-type band in the infrared spectrum of the gas with a minimum at 802 cm^{-1} is assigned to the out-of-plane SiH bending mode with the in-plane vibration as a very strong A/C-type band in the same spectrum. The two very sharp features at 844 and 583 cm^{-1} in the infrared spectrum of the solid are attributed to the A′ and A″ $(CH_2)_2$ rocks, respectively. A weak and depolarized Raman band at

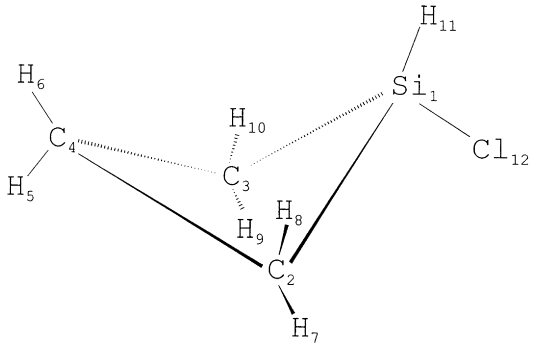

Fig. 6. Equatorial conformation of 1-chlorosilacyclobutane.

663 cm^{-1} is assigned to the A″ SiC ring stretch, whereas the corresponding A′ fundamental is observed as a doublet at 677/667 cm^{-1} in the infrared spectrum of the krypton solution for the equatorial and axial conformers, respectively. The SiCl stretches of the two conformers produce a pair of bands around 560 cm^{-1} (equatorial) and 475 cm^{-1} (axial) with the characteristic splitting for the $^{35}Cl/^{37}Cl$ isotopic species. The lower frequency band is assigned to the axial form and is not present in the spectra of the crystalline solid.

A very strong and polarized band at 399 cm^{-1} in the Raman spectrum of the liquid is assigned to the ring deformation of the equatorial conformer. The counterpart of this band for the axial form is observed at 528 cm^{-1} in the spectrum of the krypton solution. The ring puckering fundamental, which is extensively mixed with the SiCl in-plane bend, is associated with the doublet at 265/255 cm^{-1} in the far infrared spectrum of the solid and the bending vibration is at 139 cm^{-1}. Finally, the medium intense B-type band at 182 cm^{-1} in the far infrared spectrum of the gas is attributed to the SiCl out-of-plane bend.

6. Results and discussion

Since the enthalpy differences between the conformers of two other silacyclobutanes [25,26] have already been reported, it is interesting to compare them to the ΔH value obtained in this study. For 1-methylsilacyclobutane [26] and 1-chloro-1-methylsilacyclobutane [25], the equatorial conformers are more stable than the axial forms by 122 ± 26 and 178 ± 15 cm^{-1}, respectively. It should be noted that the equatorial form of 1-chloro-1-methylsilacyclobutane has the chlorine atom in the equatorial position. The same equatorial form is the more stable conformer of 1-chlorosilacyclobutane by 211 ± 17 cm^{-1} (Fig. 6). The trend in the ΔH values of the three compounds shows that the chlorine atom is most preferred in equatorial position, followed by the methyl group. This coupled with the fact that the chlorine atom and the methyl group have almost the same van der Waals radii, suggest that the electronegativity factor is more important than the steric factor for the preferred position of the substitituent. A rough estimate of the combined effect of these two factors requires that the sum of the ΔH values for 1-chloro-1-methyl- and 1-methyl-silacyclobutane (300 ± 41 cm^{-1}) is in the proximity of the ΔH value for 1-chlorosilacyclobutane (211 ± 17 cm^{-1}). The former value is slightly larger indicating that such a simple model does not account for all factors governing the conformational stability. The ab initio predicted energy difference varies with the basis sets (Table 2), but on average it is consistent with the experimental ΔH value.

There is an excellent agreement between the observed and calculated infrared spectra (Fig. 2). This fact confirms the reliability of the ΔH value obtained in the liquid krypton solution. However, the observed and calculated Raman spectra show some noticeable differences, especially in the 500–1000 cm^{-1} region. For example, in the Raman spectrum of the liquid (Fig. 5A), the C–C ring stretch (880/887 cm^{-1}) appears to be at least twice more intense than the CH_2 rock (908/921 cm^{-1}), whereas in the calculated Raman spectrum (Fig. 5B), the two fundamentals have comparable intensities. Additionally, the $(CH_2)_2$ wagging mode at 1126 cm^{-1} has much higher relative intensity in the observed spectrum compared to the predicted value in the calculated spectrum.

The potential energy distributions for the A″ fundamentals of both conformers are quite pure; however, in the A′ symmetry block, there is extensive mixing between the vibrational modes. For example, the fundamentals at 1186, 917, and 835 cm^{-1} cannot be adequately described by the names $(CH_2)_2$ twist, CH_2 rock and $(CH_2)_2$ rock, respectively, because they contain almost equal contributions from several

Table 6
Fit of the rotational constants (the A rotational constants are not as well determined as the B and C rotational constants) (MHz) from r_0 adjusted parameters listed in Table 2

Molecule	Rotational constant	Equatorial			Axial		
		Obs.	Calc.	Δ	Obs.	Calc.	Δ
c-$C_3H_6Si^{35}ClH$	A	7534.70	7536.29	1.59	5929.00	5926.73	2.27
	B	1877.93	1877.51	0.42	2082.92	2083.14	0.22
	C	1692.82	1692.54	0.28	1988.08	1988.22	0.14
c-$C_3H_6Si^{37}ClH$	A	7526.60	7527.70	1.10	5911.00	5911.96	0.95
	B	1827.98	1827.52	0.46	2030.15	2030.61	0.46
	C	1652.53	1652.22	0.31	1941.60	1941.89	0.29

modes, ranging from S_8 to S_{16}. Similarly, it is difficult to determine which of the fundamentals located at 246 and 104 cm^{-1} is the ring puckering mode and which one is the Si–Cl in-plane bend of the equatorial conformer. Similar mixing is found for many of the corresponding modes of the axial conformer.

Utilizing the Si–H stretching frequencies of 2172 and 2168 cm^{-1}, we calculated the Si–H distances (r_0) for the equatorial and axial conformers [41] to be 1.482 and 1.483 Å, respectively. These values are approximately 0.007 Å longer than the distances predicted from the MP2/6-311+G(d,p) calculations. The predicted Si–H bond distances of 1.485 and 1.486 Å for the equatorial and axial conformers, respectively from the MP2/6-31G(d) calculations are in better agreement with the above values.

Utilizing the rotational constants reported for the ^{35}Cl and ^{37}Cl isotopic species for both conformers from the microwave study of Favero et al [42], the structural parameters have been obtained for 1-chlorosilacyclobutane with a computer program described in detail elsewhere [43]. This program combines the information from the microwave experimental data and ab initio calculations, and gives structural parameters which fit the rotational constants with the structural parameters remaining close to the ab initio values. In order to reduce the number of independent variables, the structural parameters are separated into sets according to their types. For example, the six CH bond lengths for both conformers form one set and the six CCH angles for the two conformers form another set. Each set uses only one independent parameter in the optimization and all structural parameters in one set are adjusted by the same adjustment factor. The differences between the similar parameters from the ab initio calculations are retained in the final results. Bond lengths in the same set keep their relative ratio and bond angles and torsional angles in the same set keep their differences in degrees. If one CH bond is 1% longer than another CH bond by ab initio calculations, it will still be 1% longer after the optimization. If a CCH angle is 1 degree larger than another CCH angle from the ab initio calculation, it will still be 1° larger in the final result. This assumption is based on the fact that the errors from ab initio calculations are systematic. With twelve experimental rotational constants from the earlier microwave study [42], only eleven r_0 structural parameters can be obtained by combining the ab initio calculations and the microwave data. Since the Si–H distances have been obtained from the vibrational frequencies, there are only four sets of distances to be varied for the two conformers. Similar reductions can be made for the sets of angles with the expectation that the heavy atom angles will most effect the rotational constants. The program searches the minima of the function $F(k_1, k_2, \ldots)$:

$$F(k_1, k_2, \ldots) = \sum_i (100K_i)^2 + \sum_j (20K_j)^2 + \sum_l (0.1K_l)^2 + \sum_m (0.02K_m)^2$$

The adjustment factors, K, in the formula are defined as:

$$K_i = (R_{c_i} - R_{o_i})/R_{o_i}; K_j = (L_{c_j} - L_{a_j})/L_{a_j}; K_l = A_{c_l} - A_{a_l}; K_m = T_{c_m} - T_{a_m}$$

where *R*, *L*, *A* and *T* represent the rotational constants, bond lengths, bond angles and torsional angles, respectively. The lower case letters c, o, and a indicate calculated where calculated means by the A and M program, observed (rotational constants), and ab initio bond lengths, bond angles and torsional angles, respectively. The subscript runs over all structural parameters in the optimization. Only torsional angles around single bonds are considered as torsional angles in the calculations whereas other angles defined by the third internal coordinate in the ab initio input data are treated as bond angles. To avoid the possibility of falling into a local minimum instead of the global minimum of *F*, the simplex algorithm instead of the gradient method was used to optimize the adjustment factors in searching for the minimum of *F*.

Utilizing the structural parameters obtained from the MP2/6-311+G(d,p) calculation along with the knowledge that the Si–Cl distance is predicted too long from these calculations [44], the adjusted r_0 parameters listed in Table 2 were obtained. These parameters give rotational constants within 0.04% (Table 6) of those obtained from the microwave study [42]. It is believed that the errors of these parameters should be within 0.005 Å of the actual distances and 0.5° for the angles except for the puckering angle of the ring. The ab initio calculations are not going to be very sensitive to this parameter since the potential for this angle is going to be reasonably flat. In addition, this angle is strongly correlated with the Si–Cl bond distance so a longer Si–Cl bond distance than the one given in Table 2 will result in a smaller puckering angle. Thus, it is believed that these two parameters are the least certain of the adjusted r_0 values. It would be of interest to see how these parameters compare to those being obtained from an electron diffraction study [45].

The major difference in the structural parameters between the two conformers, in addition to the puckering angle, are the Si–Cl, Si–C_2(C_3) and C–H_7(H_9) distances along with some of the SiCH and CCH angles. The difference in the Si–Cl distance is 0.007 Å and the Si–C distance is 0.004 Å, which seem reasonable from the switching of the axial and equatorial atoms. The difference of 8° in the puckering angle between the two conformers is larger than expected but it is clear that the chlorine atom significantly effects the ring since the C–H_7(H_9) bond distances are 0.006 Å longer when the chlorine atom is in the axial position than in the equatorial position.

The barrier to interconversion between the conformers of 1-chlorosilacyclobutane can be estimated by ab initio energy calculation of the transition state along the puckering coordinate. Using the MP2/6-31G(d) basis set, we obtained an equatorial-to-axial barrier of 681 cm^{-1}. This value compares well to the previously reported barrier of 685 cm^{-1} for 1-methylsilacyclobutane [26]. Actually, the puckering barriers of two recently investigated, similar molecules, 1-chloro-1-methylsilacyclobutane and 1-fluoro-1-methylsilacyclobutane, have also similar magnitudes of 605 and 674 cm^{-1}, respectively. These values were obtained in this study from the MP2/6-31G(d) calculation and correspond to the barriers for transition from the more stable to the less stable conformers. The enthalpy values for conversion from the less stable to the more stable conformers of these molecules are even lower (~400 cm^{-1}). Obviously, the puckering barrier is not very sensitive to the substituents at the silicon atom. On the contrary, the experimentally determined puckering barrier in silacyclobutane [46] is 440 ± 10 cm^{-1}, which is about 30% lower than the ab initio calculated (this study, MP2/6-31G(d)) value of 612 cm^{-1}. Similarly, the experimental [2] and ab initio calculated (this study, MP2/6-31G(d)) barriers for cyclobutane are substantially different having values of 510 ± 2 and 792 cm^{-1}, respectively. The latter two comparisons suggest that the reported ab initio puckering barriers for the substituted silacyclobutanes could be overestimated by about 200 cm^{-1} at this level of calculation.

Finally, it should be noted the value of the ab initio predicted structural parameters, infrared spectrum, Raman spectrum and conformational stabilities to this experimental spectroscopic study. In the decade ahead, it is expected that more use will be made of vibrational intensities in the application of spectroscopic data for chemical information. Also when structural parameters are needed there will be more reliance on ab initio predicted parameters and fewer structural determinations by microwave and electron diffraction studies. Thus, it is important to establish the level of ab initio calculations needed to provide good r_0 predicted values for a given type of molecule.

Acknowledgements

JRD acknowledges the University of Kansas City Trustees for a Faculty Fellowship award for partial financial support of this research.

References

[1] J.M.R. Stone, I.M. Mills, Mol. Phys. 18 (1970) 631.
[2] T. Egawa, S. Yamamoto, T. Ueda, K. Kuchitsu, J. Mol. Spectrosc. 126 (1987) 239.
[3] J.R. Durig, J.F. Sullivan, D.T. Durig, Mol. Cryst. Liq. Cryst. 54 (1979) 51.
[4] G.W. Rathjens Jr., W.D. Gwinn, J. Am. Chem. Soc. 75 (1953) 5629.
[5] G.W. Rathjens Jr., J.K. Freeman, W.D. Gwinn, K.S. Pitzer, J. Am. Chem. Soc. 75 (1953) 5634.
[6] G.F. Carter, D.H. Templeton, Acta Crystallogr. 6 (1953) 805.
[7] J.D. Dunitz, V. Schomaker, J. Chem. Phys. 20 (1952) 1703.
[8] A. Almenningen, O. Bastiansen, P.N. Skancke, Acta Chem. Scand. 15 (1961) 711.
[9] E. Castellucci, M.G. Migliorani, P. Manzelli, Acta Crystallogr. A28 (1972) 432.
[10] J.R. Durig, A.C. Morrisey, J. Chem. Phys. 46 (1966) 4854.
[11] J.R. Durig, W.H. Green, J. Chem. Phys. 47 (1967) 673.
[12] J.R. Durig, J.N. Willis Jr., W.H. Green, J. Chem. Phys. 54 (1971) 1547.
[13] C.S. Blackwell, L.A. Carreira, J.R. Durig, J.M. Karriker, R.C. Lord, J. Chem. Phys. 56 (1972) 1706.
[14] J.R. Durig, L.A. Carreira, J.N. Willis, J. Chem. Phys. 57 (1972) 2755.
[15] J.R. Durig, A.C. Shing, L.A. Carreira, J. Mol. Struct. 17 (1973) 423.
[16] J.R. Durig, T.J. Geyer, T.S. Little, V.F. Kalasinsky, J. Chem. Phys. 86 (1987) 545.
[17] V.F. Kalasinsky, W.C. Harris, P.W. Holtzclaw, T.S. Little, T.J. Geyer, J.R. Durig, J. Raman Spectrosc. 18 (1987) 581.
[18] J.R. Durig, T.S. Little, M.J. Lee, J. Raman Spectrosc. 20 (1989) 757.
[19] J.R. Durig, M.J. Lee, T.S. Little, J. Raman Spectrosc. 21 (1990) 529.
[20] J.R. Durig, M.J. Lee, T.S. Little, Struct. Chem. 2 (1991) 195.
[21] J.R. Durig, M.J. Lee, W. Zhao, T.S. Little, Struct. Chem. 3 (1992) 329.
[22] G.W. Rothschild, B.P. Dailey, J. Chem. Phys. 36 (1962) 2931.
[23] H. Kim, W.D. Gwinn, J. Chem. Phys. 44 (1966) 865.
[24] W. Caminati, L.B. Favero, A. Maris, P.G. Favero, J. Mol. Struct. (2000) in press.
[25] T.K. Gounev, G.A. Guirgis, T.A. Mohamed, P. Zhen, J.R. Durig, J. Raman Spectrosc. 30 (1999) 399.
[26] J.R. Durig, P. Zhen, Y. Jin, T.K. Gounev, G.A. Guirgis, J. Mol. Struct. 477 (1999) 31.
[27] G.A. Guirgis, T.K. Gounev, P. Zhen, J.R. Durig, Spectrochim. Acta 55 (1999) 2753.
[28] J. Laane, J. Am. Chem. Soc. 89 (1967) 1144.
[29] F.A. Miller, B.M. Harney, Appl. Spectrosc. 24 (1970) 291.
[30] M.J. Frisch, G.W. Trucks, H.B. Schlegel, P.M.W. Gill, B.G. Johnson, M.A. Robb, J.R. Cheeseman, T.A. Keith, G.A. Petersson, J.A. Montgomery, K. Raghavachari, M.A. Al-Laham, V.G. Zakrzewski, J.V. Ortiz, J.B. Foresman, J. Cioslowski, B.B. Stefanov, A. Nanayakkara, M. Challacombe, C.Y. Peng, P.Y. Ayala, W. Chen, M.W. Wong, J.L. Andres, E.S. Replogle, R. Gomperts, R.L. Martin, D.J. Fox, J.S. Binkley, D.J. Defrees, J. Baker, J.P. Stewart, M. Head-Gordon, C. Gonzalez, J.A. Pople, GAUSSIAN 94 (Revision B. 3), Gaussian Inc., Pittsburgh, PA, 1995.
[31] P. Pulay, Mol. Phys. 17 (1969) 197.
[32] M.J. Frisch, Y. Yamaguchi, J.F. Gaw, H.F. Schaefer III, J.S. Binkley, J. Chem. Phys. 84 (1986) 531.
[33] R.D. Amos, Chem. Phys. Lett. 124 (1986) 376.
[34] P.L. Polavarapu, J. Phys. Chem. 94 (1990) 8106.
[35] G.W. Chantry, in: A. Anderson (Ed.), The Raman Effect, vol. 1, Marcel Dekker, New York, 1971 (chap. 2).
[36] W.A. Herrebout, B.J. van der Veken, A. Wang, J.R. Durig, J. Phys. Chem. 99 (1995) 578.
[37] W.A. Herrebout, B.J. van der Veken, J. Phys. Chem. 100 (1996) 9671.
[38] M.O. Bulanin, J. Mol. Struct. 19 (1973) 59.
[39] M.O. Bulanin, J. Mol. Struct. 347 (1995) 73.
[40] B.J. van der Veken, E.R. DeMunck, J. Chem. Phys. 97 (1997) 3060.
[41] J.L. Duncan, J.L. Harvie, D.C. Mckean, S. Cradock, J. Mol. Struct. 145 (1986) 225.
[42] L.B. Favero, G. Maccaferni, W. Caminati, M. Grosser, M. Dakkouri, J. Mol. Struct. 176 (1996) 321.
[43] B.J. van der Veken, W.A. Herrebout, D.T. Durig, W. Zhao, J.R. Durig, J. Phys. Chem. 103 (1999) 1976.
[44] J.R. Durig, Y.E. Nashed, M.A. Qtaitat, G.A. Guirgis, submitted for publication.
[45] M. Dakkouri, private communication.
[46] J. Laane, R.C. Lord, J. Chem. Phys. 48 (1968) 1508.